Supplementary Materials for

Targeting latency-associated peptide promotes anti-tumor immunity

Galina Gabriely[1], Andre P. da Cunha[1,2], Rafael M. Rezende[1], Brendan Kenyon[1], Asaf Madi[1], Tyler Vandeventer[1], Nathaniel Skillin[1], Stephen Rubino[1], Lucien Garo[1], Maria A. Mazzola[1], Panagiota Kolypetri[1], Amanda J. Lanser[1], Thais Moreira[3], Ana Maria C. Faria[3], Hans Lassmann[4], Vijay Kuchroo[1], Gopal Murugaiyan[1] and Howard L. Weiner[1]*

*Corresponding author. Email: hweiner@rics.bwh.harvard.edu

This PDF file includes:

Materials and Methods

Cell lines

B16F10, CT26, and MC38 cell lines were purchased from ATCC. GL261 cell line was purchased from NIH. GL261-OVA cell line was a gift from M. Olin (49). B16-OVA cell line was provided by C. Sedlik, Institut Curie. P3U1 cell line expressing mouse TGF-β1 (P3U1-TGF-β1) was generated in our lab by T. Oida as previously described (14).

Tumor implantation

In preparation for subcutaneous injections, cultured tumor cell lines (B16F10, GL261, MC38, CT26) were washed twice in PBS, counted and diluted to a desired concentration in PBS. B16F10, GL261, and MC38 tumors were implanted in 8-10 weeks of age male WT C57BL/6 mice and CT26 tumors were implanted in 8-10 weeks of age male WT BALB/c mice. Each mouse was implanted with 5×10^5 (B16F10, CT26, or MC38) - 1×10^6 (GL261) cells by subcutaneous injections into the animal's right flanks. Tumor size was measured in two dimensions (length, L and width, W) by caliper and tumor volumes were calculated according to the following formula: Tumor volume=0.5 x (L x W^2). Intracranial tumors were implanted with either GL261 or GL261-OVA stereotactically, 1×10^5 cells into the right striatum; coordinates were 2 mm lateral, 0.5 mm anterior of bregma, and 3 mm deep from the cortical surface of the brain.

AOM/DSS Model of Colorectal Carcinoma

Mice were treated with 10 mg/kg of azoxymethane (AOM), administered i.p. on day 0. A week later, mice were treated with three cycles of one week 2.5% Dextran Sulfate Sodium Salt (DSS) in the drinking water, followed by two weeks normal drinking water. At the end of the last DSS cycle, drinking water was resumed until the termination of the

experiment. Mice were treated with either anti-LAP or IC initially weekly and after the last DSS treatment every three days (10 mg/kg). Seventy-seven days after the administration of AOM, mice were sacrificed and tumor number and size were measured.

Adoptive transfer

Cd8a^{tm1Mak} (CD8KO) mice were adoptively transferred with PBS, CD103+ CD8 T cells, CD103- CD8 T cells or a mix of 1:1 CD103+ and CD103- CD8 T cells isolated from melanoma-bearing mice or naïve mice on days -1 and 8. A total of 1-2 × 10^6 cells was mixed in PBS and injected i.v. (tail veins). One day after first cell transfer (day 0), mice were implanted with B16 melanoma cells (5 × 10^5 cells per mouse) and tumor growth was followed by caliper measurements.

DC Vaccination

DCs were derived from bone marrow as previously described (50) and cultured in complete medium (RPMI 1640 medium, 10% FBS, 50 μM 2-Mercaptoethanol, 10 ng/mL IL-4, and 20 ng/mL GM-CSF). On day 7, DCs were pulsed for 24 h with 100 μg/ml ovalbumin (OVA, InvivoGen). OVA-loaded DCs were collected, washed and resuspended in PBS. Mice were vaccinated by subcutaneous injections (s.c.) of 2 x 10^6 dendritic cells/mouse.

Flow cytometry staining and acquisition

Immune cells were isolated from lymphoid organs (and in some cases from tumors). Cells were prepared in FACS buffer (HBSS containing 2% FBS, 2 mM EDTA, and 25 mM HEPES) and blocked with anti-mouse CD16/CD32 (1:50) for 15 minutes on ice to

block the Fc receptors. Cells were then stained with the indicated fluorochrome-labeled antibodies purchased from eBioscience, BioLegend or BD Pharmingen. For intracellular cytokine staining, cells were stimulated for 4 h with PMA (phorbol 12-myristate 13-acetate; 50 ng/ml; Sigma), ionomycin (1 μg/ml; Sigma) and monensin (GolgiStop; 2-μM BD Biosciences). After staining of surface markers, cells were fixed and made permeable with Foxp3 Fixation/Permeabilization (eBiosceince) according to the manufacturer's instructions and stained with Abs against cytokines. The following Abs against surface molecules were used: CD4 (clone RM4-5), CD8 (clone 53-6.7), CD3 (clone 145-2C11), NK1.1 (clone PK136), CD11b (clone M1/70), CD11c (clone N418), MHCII (clone M5/114.15.2), CD86 (clone GL1), CD44 (clone IM7), CD103 (clone 2E7), mouse LAP (clones TW7–16B4 or TW7-28G11), Lag3 (clone C9B7W), Tim3 (clone RMT3-23), CTLA4 (clone UC10-4B9), KLRG1 (clone 2F1), KLRA7/Ly-49G (clone 4D11), IL-2Rb (clone TM-b1), IL18-R1 (clone P3TUNYA), CD107 (clone 1D4B), IL7R/CD127 (clone A7R34), CD62L (clone MEL14), H-2Kb OVA Pentamer (ProImmune, clone 1122), PD-L1 (clone MIH5), and PD-1 (clone RMP1-30). Fixable viability dye eF506 (eBioscience) was used to exclude dead cells. For intracellular staining, cells were stained with Abs against IL-2 (clone JES6-5H4), IL-10 (clone JES5-16E3), TNF-α (clone MP6-XT22), IFN-γ (clone XMG-1.2), Foxp3 (clone FJK-16s), Ki-67 (clone SolA15), Eomes (clone 64.5), Granzyme A (clone 159.5) or Granzyme B (clone NGZB). Samples were analyzed on the LSRII or Fortessa flow cytometers (BD Biosciences), data was analyzed using the FlowJo software (Tree Star, Ashland, OR, USA).

DC and T cell co-culture assay

Splenocytes were harvested, CD11c-Hi and CD11c-Int cell subsets were sorted and cells were cultured at 1:8 (CD11c:CD8) ratio with CD8+ naïve T cells 100, 000 cells/well

in 96-well plate isolated with a selection kit (Miltenyi Biotec) according to the manufacturer's protocol, sorted and stained with CellTrace Violet (Invitrogen). At day 3, cell culture supernatants were collected for cytokine assay with Mouse Cytokine/Chemokine Magnetic Bead Panel (Millipore Cat # MCYTOMAG) and as instructed in the user manual and CD8+ T cell viability analyzed with a 7AAD staining by flow cytometry.

TGF-β enzyme-linked immunosorbent assay (ELISA)

P3U1-TGF-β1 cells were maintained in DMEM supplemented with 10% FBS, 1 mM Sodium Pyruvate, 55 μM 2-betamercaptoethanol, 5.5 mM L-Glutamine, 1,000 U/ml Penicillin/Streptomycin medium. For anti-LAP blocking assay, cells were washed twice in DMEM serum-free media described above and plated in U-bottom 96-well plate at 40, 000 cells/well in 250 μl of serum-free media to remove residual TGF-β from fetal bovine serum. These cells were treated with anti-LAP clones or isotype control antibody at a concentration of 250 μg/ml. The cells were then incubated for 48 h and cell-free culture supernatants collected for cytokine measurement. ELISA was performed by using TGF-beta 1 Quantikine ELISA Kit according to the manufacturer's instructions (MB100B; R&D Systems). Briefly, the quantitative sandwich enzyme immunoassay technique with capture anti-TGF-β antibodies and detection mouse anti-TGF-β antibodies followed with anti-mouse HRP-conjugated antibody and colorimetric detection after activation with substrate.

***In vitro* suppression assay**

For LAP+ CD4 T cells: Naive CD4+ T cells (CD4+CD44^{lo}CD62L^{hi}Foxp3-) were isolated with anti-CD4 beads (Miltenyi Biotec), purified by flow cytometry from the spleen and

lymph nodes of Foxp3-GFP mice, stained with CellTrace Violet according to the manufacturers' recommendation (CellTrace Violet proliferation kit, Invitrogen) and used as responder cells. Naive T cells, 50,000-100,000 cells per well of 96-well plate, were stimulated with anti-CD3 (0.5 μg/ml; 14-0031-86; eBioscience) in the presence of DCs (1:16 ratio). For suppression assays, sorted LAP+CD4+ or Foxp3+CD4+ cells were isolated from tumor-bearing mice cells and cultured at 1:1 ratio with responder cells in the presence of DCs in IMDM medium supplemented with 10% FBS in 96-well round-bottom plates. In some experiments, 10 μM of TGF-β receptor inhibitor, 50 μg of anti-TGF-β (1D11.16.8) blocking antibody or IC antibody per well were added. Proliferation was assessed 72 h later by flow cytometry, based upon the dilution of the CellTrace violet dye.

For CD103+ CD8 T cells: Naive CD8+ T cells ($CD8+CD44^{lo}CD62L^{hi}CD25-$) were purified by flow cytometry from the spleen and lymph nodes of unimmunized WT mice, stained with CellTrace Violet according to the manufacturers' recommendation (Invitrogen) and used as responder cells. Naive T cells were stimulated with anti-CD3 (0.25 μg/ml; 14-0031-86; eBioscience) in the presence of DCs. For suppression assays, CD103+ CD8 T cells were isolated from naïve or tumor-bearing mice, sorted and cultured (50,000-100,000 cells per well of 96-well plate) at 1:1 ratio with responder cells in the presence DCs (1:16 ratio) in IMDM medium supplemented with 10% FBS in 96-well round-bottom plates. In some experiments, 50 μg/well of anti-PD1 (RMP-1), anti-PD-L1 (10F.9G2) or IC blocking antibodies were added. Proliferation was assessed 48 h later by flow cytometry, based upon the dilution of the CellTrace violet dye.

Dendritic cell isolation for suppression assay: DCs were isolated from spleen treated with HBSS containing Collagenase D (1 mg/mL) and DNase (20 μg/mL), sliced and incubated at 37^{o}C for 45 min. After neutralization with FBS and wash, dendritic cells were enriched using the CD11c+ selection kit (Miltenyi Biotec) according to the manufacturer's protocol. DCs were plated at 1:16 ratio with responder cells.

nCounter gene expression and analysis

Total RNA was isolated from sorted T cells using the miRNeasy Kit (Qiagen) following the manufacturer's protocol, including the optional on-column DNase Digestion step. RNA was concentrated in a SpeedVac and then used for Nanostring analysis. 100 ng of total RNA was hybridized with reporter and capture probes for nCounter Gene Expression analysis (Pan Cancer Immunology code set), according to manufacturer's instructions (NanoString Technologies). Expression values were normalized by first adjusting each sample based on its relative value to all samples. This was followed by subtracting the calculated background (mean.2sd) from each sample with additional normalization by housekeeping geometric mean, where housekeeping genes were defined as: Rpl19, Abcf1, G6pdx, Oaz1, Eef1g, Ppia, Eif2b4, Polr1b, Edc3, Hprt, Tubb5, Sf3a3, Polr2a, Tbp, Nubp1, Hdac3, Alas1, Sap130, Gusb, Sdha. Differentially expressed genes were defined using the function that fits multiple linear models from the Bioconductor package limma in R (51). Transcriptional profiling was performed on three samples per group and each of these samples was a collection of cells from 3-8 mice.

qRT-PCR

RNA was extracted with miRNAeasy kit (Qiagen, USA) following the manufacturer's protocol, including the optional on-column DNase Digestion step. cDNA was prepared by using the Reverse-Transcription PCR Kit following the manufacturer's instructions

(Applied Biosystems, USA) and used for qPCR, and the results were normalized to *Gapdh* or *B2m*. All the primers and probes were provided by Applied Biosystems, and were used on the ViiA 7 Real-Time PCR System (Applied Biosystems). *Gapdh* (Mm00484668_m1), *Tigit* (Mm03807522_m1), *Lag3* (Mm00493071_m1), *Vcam* (Mm01320970_m1), *Irf4* (Mm00516431_m1), *Tgfb1* (Mm01178820_m1), *Il10* (Mm00439614_m1), *Il12* (Mm00434165_m1). For detection of *Il10, Tgfb1* and *Il12*, DC subsets were stimulated 4 hours *in vitro* with 3 μg/ml of anti-CD40 or 100 ng/ml of LPS.

Supplementary Figures

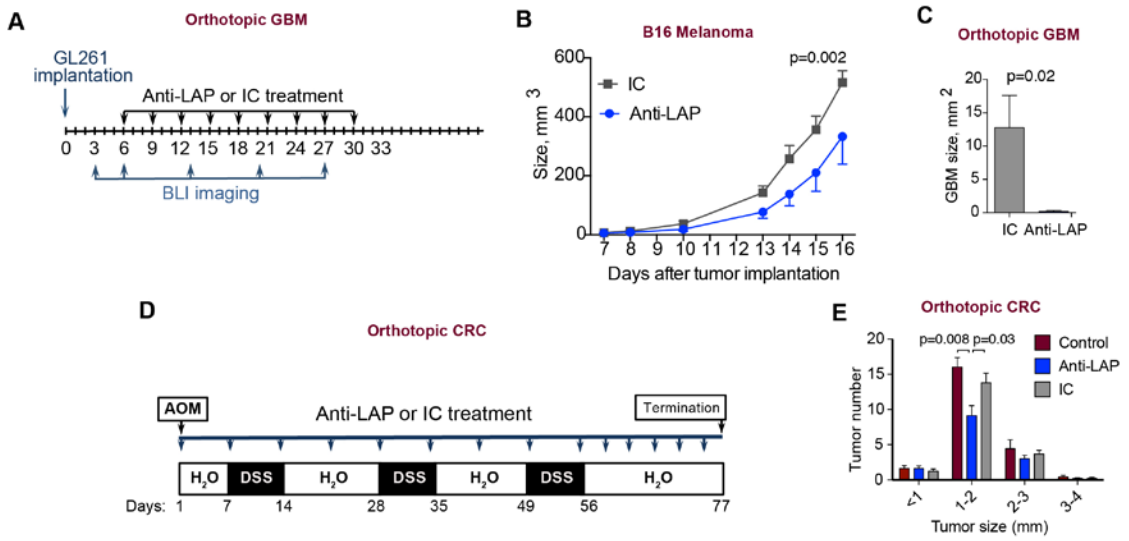

Figure S1. Effects of anti-LAP in tumor models.

(**A**) Schematic representation of experimental design for the intracranial GBM model. (**B**) Tumor growth over time of established B16 tumors treated with anti-LAP. Treatment was initiated on day 7 (when tumors became palpable) after B16 melanoma cell implantation (*n*=10 (anti-LAP) and *n*=9 (IC); two-way ANOVA; p value for the last time point is shown). (**C**) Early therapeutic effect of anti-LAP on intracranial GL261 GBM. GBM tumor sizes measured by immunohistochemistry (*n*=5; two-tailed *t*-test). (**D**) Schematic representation of experimental design for the AOM/DSS CRC model. (**E**) Orthotopic AOM/DSS induced CRC tumor number grouped by size in C57BL/6 WT mice (*n*=9 (anti-LAP and IC) and *n*=5 (control); one-way ANOVA). Error bars, mean±s.e.m.

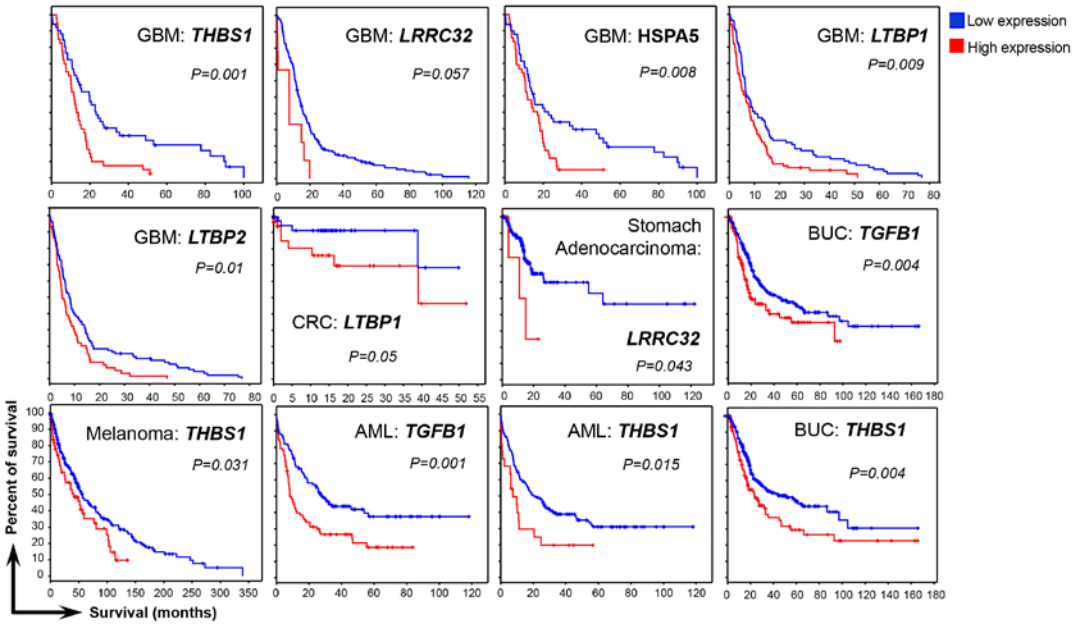

Figure S2. Expression of LAP associated genes correlates with decreased patient survival in human cancer.

Relationship between cancer patient survival and mRNA expression of LAP related genes in tumors based on The Tumor Cancer Genome Atlas (TCGA) dataset analysis. Significant correlations for THBS1/TSP-1, LRRC32/GARP, HSPA5/GRP78, and LTBP1/2 mRNAs in GBM patients, for LTBP1 gene in colorectal carcinoma (CRC), for LRRC32/GARP in stomach adenocarcinoma, TGFB1/TGF-β1 and THBS1/TSP-1 in bladder urothelial carcinoma (BUC), for THBS1/TSP-1 in melanoma, for TGFB1/TGF-β1 and THBS1/TSP-1 in acute myeloid leukemia (AML) are shown. The graphs and p values were generated and downloaded from cBioPortal (http://www.cbioportal.org) (52, 53).

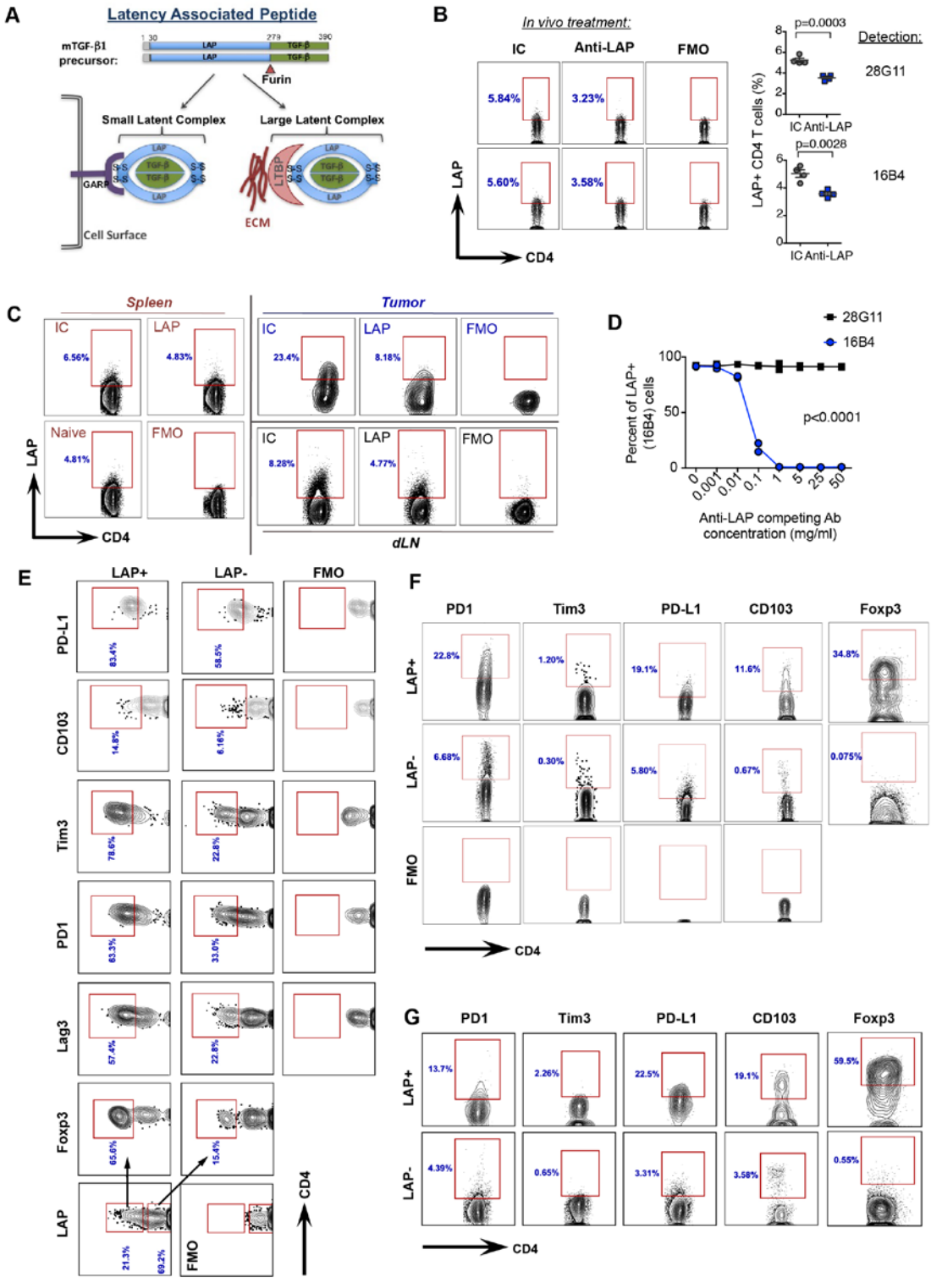

Figure S3. Analysis of LAP+ CD4 T cells in B16 melanoma model.

(**A**) Schematic presentation of LAP/TGF-β complexes. (**B**) Depletion of LAP+ CD4 T cells following anti-LAP treatment. Melanoma-bearing mice were treated with anti-LAP TW7-28G11 clone, spleens collected and the frequency of LAP+ CD4 T cells measured with anti-LAP clone TW7-28G11 and a non-competing anti-LAP clone TW7-16B4, by flow cytometry (*n*=4; two-tailed *t*-test). Representative dot plots and quantification of LAP+ cells are presented. Data are representative of at least three independent experiments. (**C**) Frequency of LAP+ CD4 T cells in spleen, dLNs and tumor from B16 melanoma mice treated with IC or anti-LAP analyzed by flow cytometry. (**D**) Competition assay between TW7-28G11 and TW7-16B4 clones of anti-LAP. P3U1 cells over-expressing mouse LAP/TGF-β were treated with indicated doses of either TW7-28G11 or TW7-16B4 antibodies for 15 minutes followed by detection with the TW7-16B4 clone of anti-LAP conjugated to APC by flow cytometry. Percent of LAP positive cells by TW7-16B4 in response to the treatment is shown (*n*=2; two-way ANOVA; p value for the last time point is shown). (**E**) Representative flow cytometry plots demonstrating immune gene (Foxp3, Lag3, PD1, Tim3, CD103, and PD-L1) expression in LAP+ vs LAP- CD4 T cells in B16 melanoma tumor. (**F**) Representative flow cytometry plots demonstrating immune gene (PD1, Tim3, PD-L1, CD103, and Foxp3) expression in LAP+ vs LAP- CD4 T cells in spleens of B16 melanoma bearing mice. (**G**) Representative flow cytometry plots demonstrating immune gene (PD1, Tim3, PD-L1, CD103, and Foxp3) expression in LAP+ vs LAP- CD4 T cells in dLNs of B16 melanoma bearing mice. Error bars, mean±s.e.m.

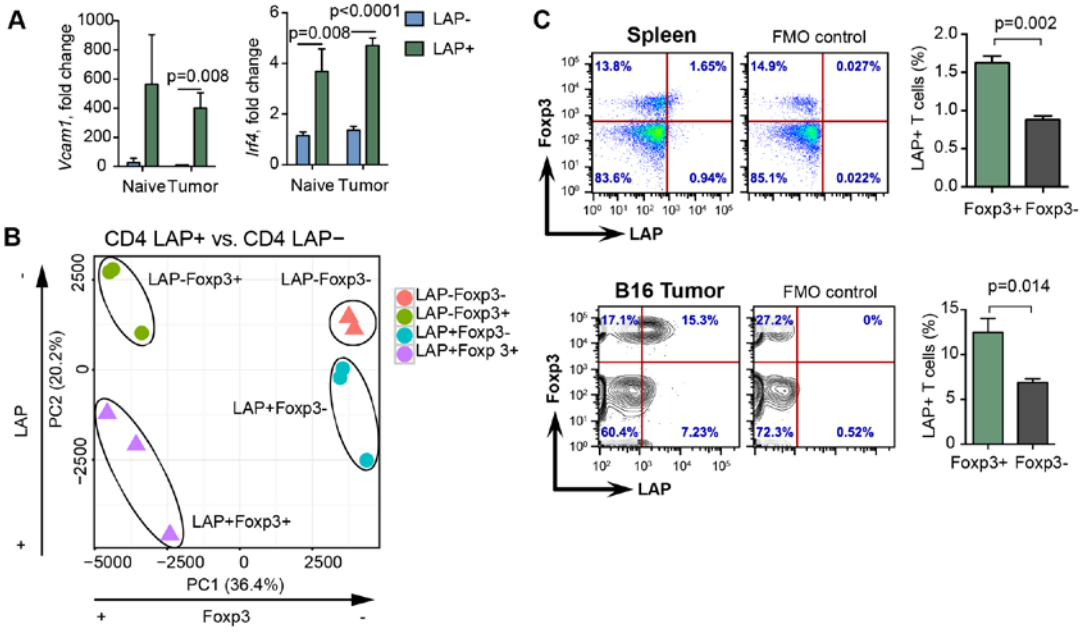

Figure S4. Analysis of LAP+ CD4 T cells in B16 melanoma model (continued).

(**A**) qRT-PCR analysis of *Vcam1* and *Irf4* on LAP+ and LAP- CD4 T cells isolated from naïve or B16 tumor-bearing mice (*n*=3). (**B**) PCA analysis of the global gene expression profile (750 genes) of LAP+Foxp3+, LAP+Foxp3-, LAP-Foxp3+ and LAP-Foxp3- cells. (**C**) Expression of LAP and Foxp3 on CD4+ T cells in spleen (upper panels) and B16 melanoma (lower panels); *n*=3. Representative dot plots and quantification are shown. Error bars, mean±s.e.m. Two-tailed *t*-test was used for p value calculations.

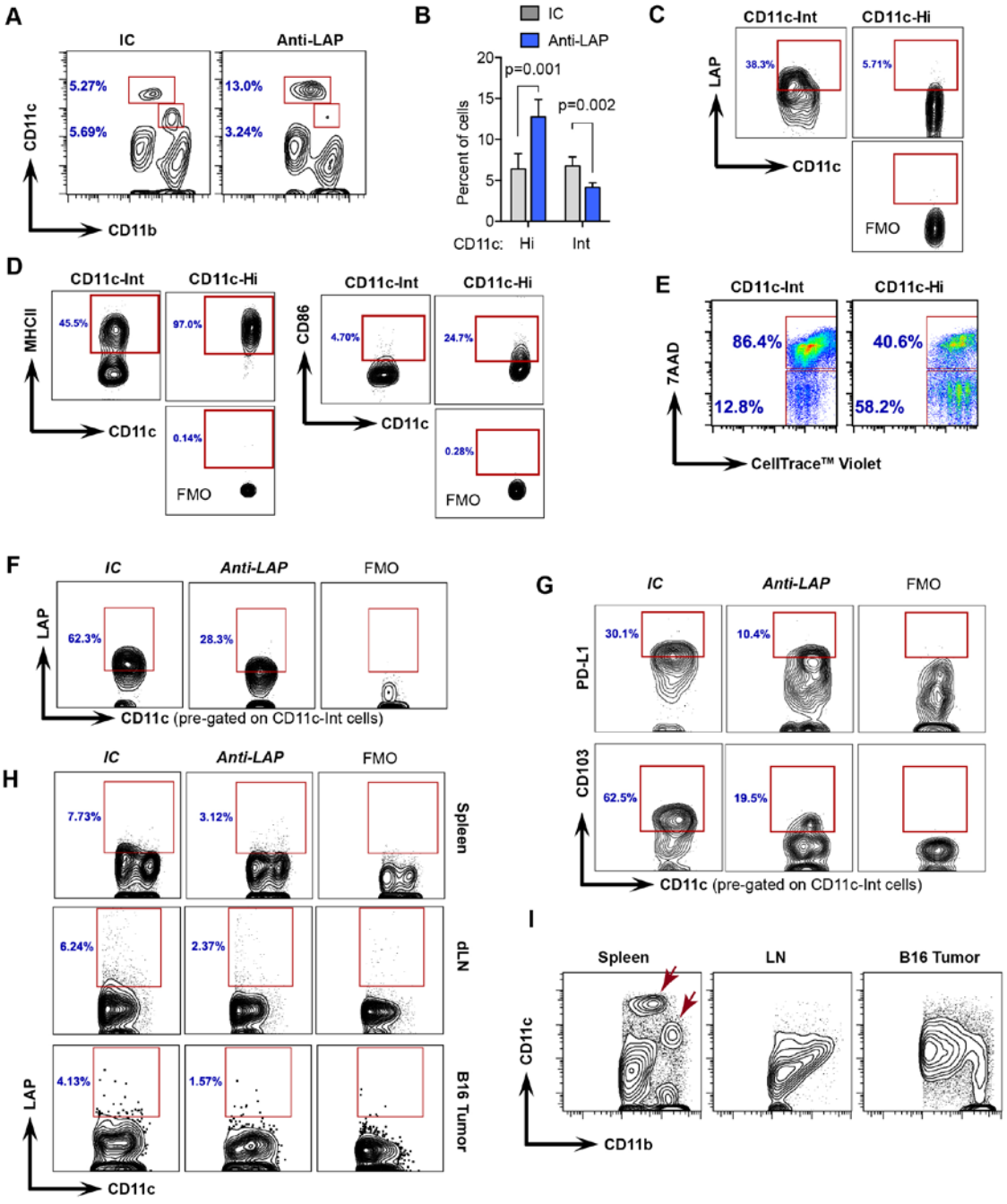

Figure S5. Immune responses by myeloid cells following anti-LAP treatment in cancer models.

(**A, B**) Effect of anti-LAP treatment on CD11c-Hi/CD11b-Int and CD11c-Int/CD11b-Hi DC populations in spleen in GL261 GBM-bearing mice by flow cytometry (shown as contour dot plots (**A**) and quantified as cell frequencies (**B**, *n*=5; two-tailed *t*-test). Data are

representative of at least two independent experiments. (**C**) Representative flow cytometry plots demonstrating LAP expression on CD11c-Hi and CD11c-Int DCs. (**D**) Representative flow cytometry plots showing MHCII and CD86 expression on CD11c-Hi and CD11c-Int DCs. (**E**) The viability of CD8+ T cell in the presence of CD11c-Int and CD11c-Hi cells *ex vivo*. CD8+ T cells were isolated, labeled with CellTrace^{TM} Violet and co-cultured with either CD11c-Int or CD11c-Hi at a ratio of 1:8 (CD11c:CD8) for three days and analyzed by flow cytometry. Representative dot plot graphs are presented. (**F**) Expression of LAP on CD11c-Int cells from spleen, following anti-LAP treatment. Representative contour dot plots are presented. (**G**) Expression of PD-L1 and CD103 on CD11c-Int cells from spleen, following anti-LAP treatment. Representative contour dot plots are presented. (**H**) Expression of LAP on CD11c+ cells from spleen, dLNs and tumor of B16 tumor-bearing mice following anti-LAP treatment. Representative contour dot plots are presented. (**I**) Analysis of CD11c-Hi/CD11b-Int and CD11c-Int/CD11b-Hi DC populations in spleen, inguinal LN (iLN) and B16 tumor by flow cytometry. Representative contour dot plots are shown. Error bars, mean$\pm$s.e.m.

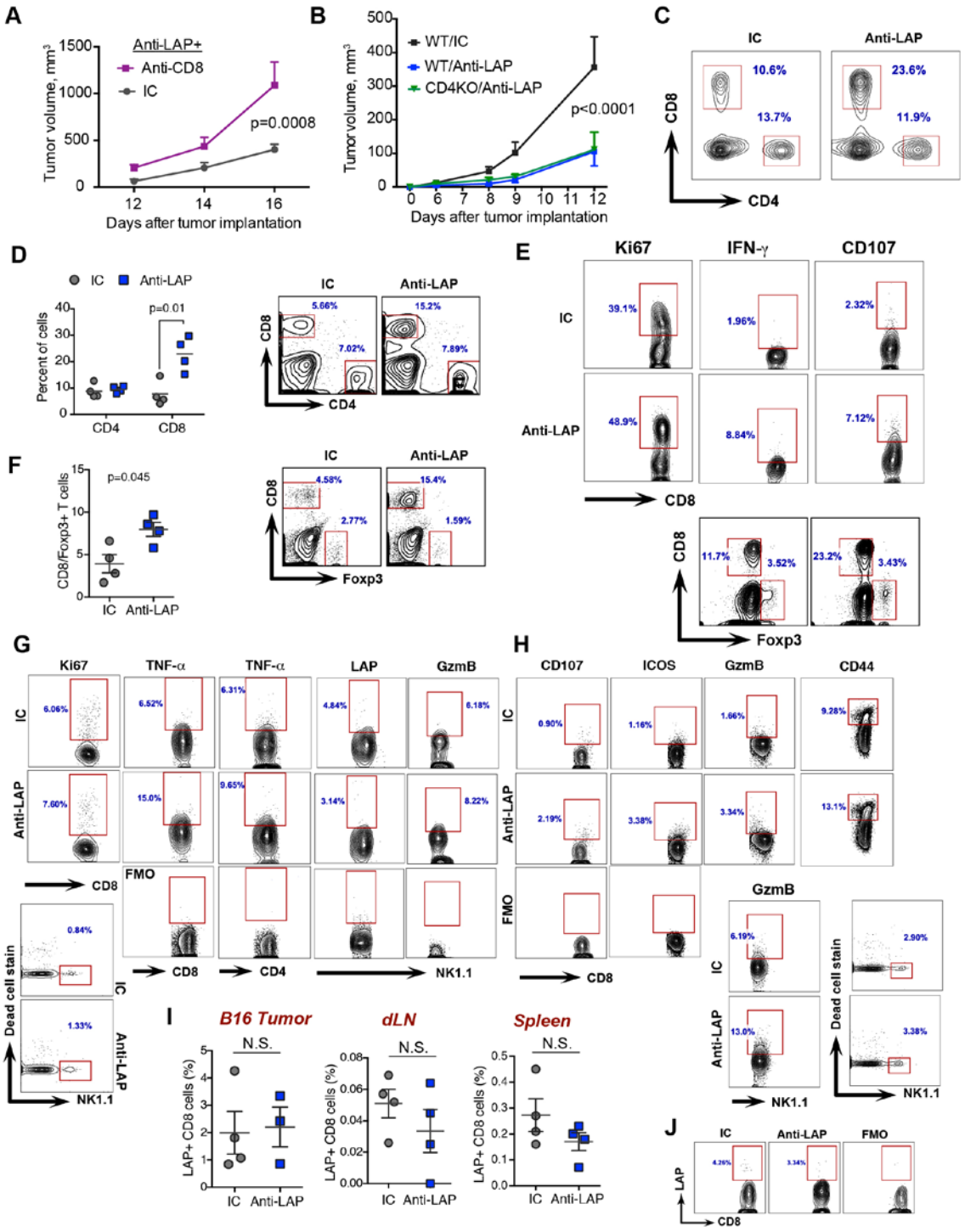

Figure S6. Immune responses following anti-LAP treatment in cancer models.

(**A**) Tumor volumes of B16 melanoma implanted mice and treated with anti-CD8 plus anti-LAP (*n*=5). (**B**) Tumor growth in WT and CD4KO mice implanted with B16 melanoma cells and treated with either anti-LAP or IC antibodies (*n*=4). Data are

representative of two independent experiments. (**C**) CD4+ and CD8+ T cells in B16 melanoma tumors following anti-LAP treatment. Representative contour dot plots are presented. (**D**) CD4+ and CD8+ T cells in GL261 GBM tumors following anti-LAP treatment. Representative contour dot plots and quantification are shown. (**E**) Analysis of tumor-infiltrating CD8+ T cells by flow cytometry. Representative FACS dot plots are presented. Bottom panels show representative plots for the ratio of CD8+ T cells/Tregs. (**F**) Ratio of CD8+ T cells/Tregs in the GL261 GBM model after anti-LAP treatment and representative plots are shown (*n*=4). (**G**) Analysis of the immune response in dLNs by flow cytometry. Representative FACS dot plots are shown. (**H**) Analysis of the immune response in spleen by flow cytometry. Representative FACS dot plots are shown. (**I, J**) LAP expression on CD8+ T cells in B16 melanoma, dLN and spleen by flow cytometry. Quantification (*n*=3-4; **I**) and representative dot plot from tumor (**J**) are shown. Error bars, mean±s.e.m. Two-way ANOVA (A and B) and two-tailed *t*-test (D, F, and I) were used for p value calculations. P values for the last time points are shown.

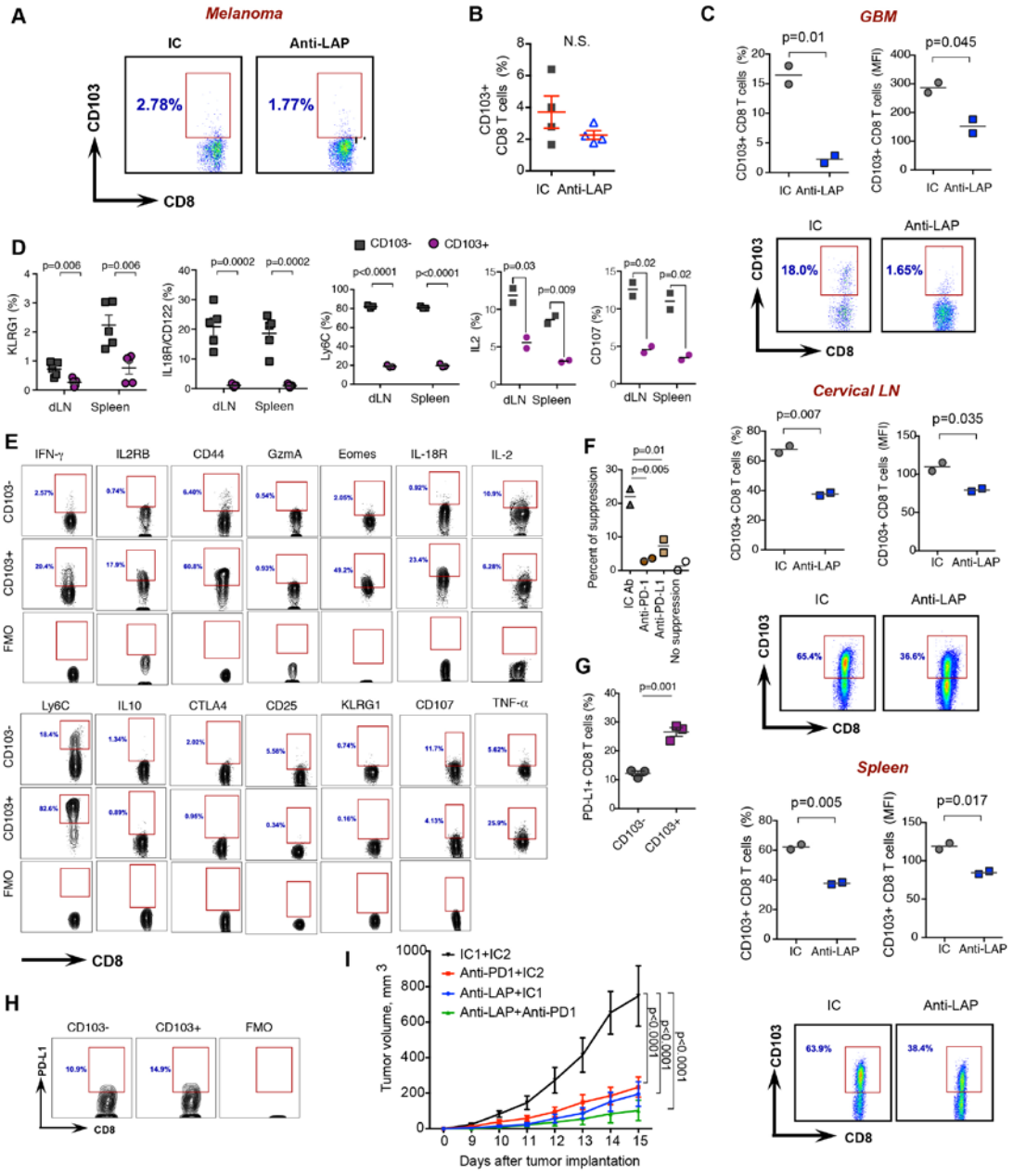

Figure S7. Effect of anti-LAP on CD103+ CD8 T cells in cancer models.

(**A, B**) CD103+ CD8 T cell infiltration into B16 melanoma following anti-LAP treatment. Dot plots (**A**) and quantification (**B**, *n*=4) are presented. (**C**) CD103+ CD8 T cells following anti-LAP treatment in the GL261 intracranial GBM model in tumor, cervical LNs and spleen. Dot plots and quantification are presented (*n*=2). (**D**) Phenotypic characterization of CD103+ and CD103- CD8 T cells in dLN and spleen of B16

melanoma-bearing mice by flow cytometry. Quantification for expression of KLRG1, IL18R, Ly6C, IL2, and CD107 on CD103+ CD8 T cells by flow cytometry is shown (*n*=2-5). (**E**) Phenotypic characterization of CD103+ and CD103- CD8 T cells in dLN of B16 melanoma-bearing mice by flow cytometry. Representative FACS dot plots for indicated genes are shown. Note: expression of these genes is similar in spleen. (**F**) Percent of suppression by CD103+ CD8 T cells in the presence of blocking antibodies against PD-1 and PD-L1 (*n*=2). (**G, H**) Expression of PD-L1 on CD103+ and CD103- CD8 T cells co-cultured with naïve CD8+ T cells and DCs for 48 h. Quantification (**G**) and representative FACS plots (**H**) are shown (*n*=3). Data were combined from two out of at least three independent experiments. (**I**) Therapeutic effect of anti-PD1 and anti-LAP against B16 melanoma. WT mice were implanted with melanoma and treated with anti-LAP and anti-PD1; anti-LAP or anti-PD1, combined with corresponding IC; or combined IC antibodies. Tumor volumes were calculated and plotted (*n*=5). Error bars, mean±s.e.m. Two-tailed *t*-test (B, C, D, and G), one-way ANOVA (F) and two-way ANOVA (I) and were used for p value calculations. P value for the last time point is shown.

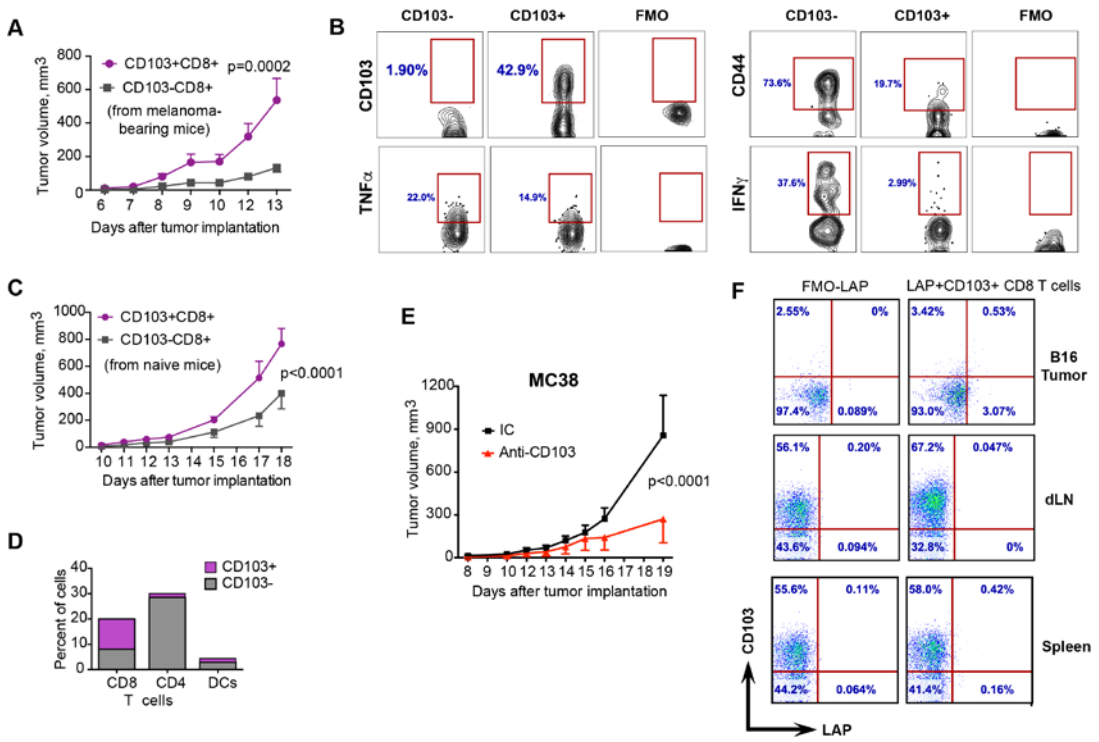

Figure S8. Characterization of CD103+ CD8 T cells in cancer models.

(**A**) B16 melanoma tumor growth after adoptive transfer of CD103+ CD8 T cells from B16 melanoma bearing mice as compared to CD103- CD8 T cells to CD8KO mice (*n*=5). (**B**) Expression of CD103, CD44, TNF-α and IFN-γ in mice from (**A**) by flow cytometry. Representative plots are shown. (**C**) B16 melanoma tumor growth after adoptive transfer of CD103+ CD8 T cells from naïve mice as compared to CD103- CD8 T cells to CD8KO mice (*n*=4 (CD103+) and *n*=5 (CD103-)). (**D**) Schematic presentation of expression of CD103 on CD8, CD4 T cells and DCs in mouse spleen. (**E**) Tumor volumes measured over time in MC38 CRC model treated with anti-CD103 (clone M290, *n*=5). (**F**) Analysis of LAP and CD103 expression on CD8+ T cells in B16 melanoma tumor, dLN and spleen by flow cytometry. Representative dot plots are shown. Error bars, mean±s.e.m. Two-way ANOVA (A, C and E) was used for p value calculations. P value for the last time point is shown.

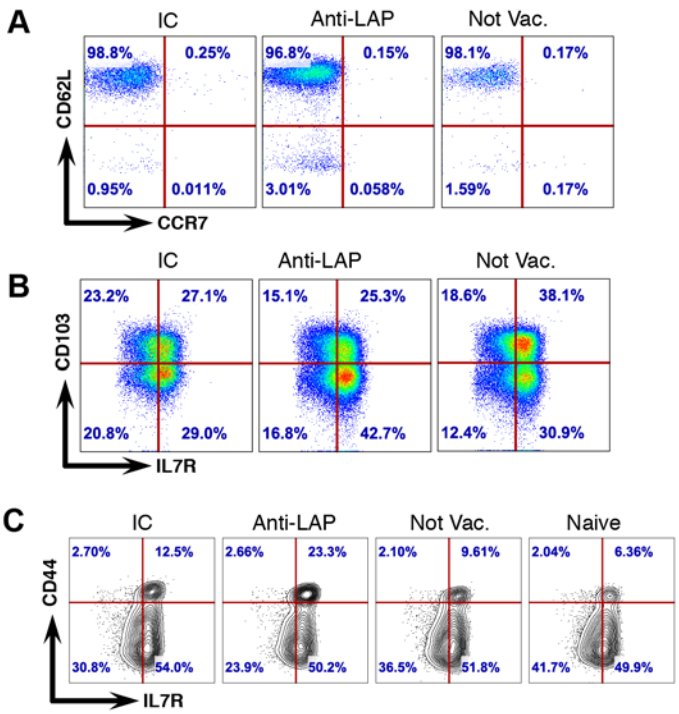

Figure S9. Anti-LAP treatment combined with antigen specific vaccination improves immune memory. (**A**) Percentage of memory-like CD8+ T cells, based on CCR7 and CD62L expression in anti-LAP treated mice. (**B**) Percentage of IL7R+CD103- CD8 T cells in anti-LAP treated mice. (**C**) Percentage of memory-like CD8+ T cells, based on CD44 and IL7R expression in anti-LAP treated mice. Representative flow cytometry dot plots are shown for vaccinated mice treated with either anti-LAP or IC, not vaccinated mice (not vac.) and naïve mice (for **C**).

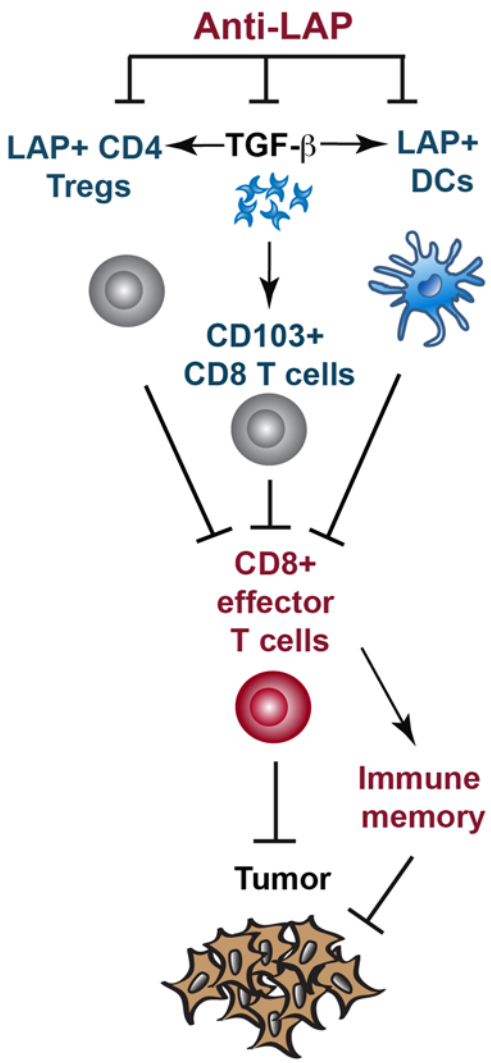

Figure S10. Schematic: Anti-LAP suppresses tumor growth by targeting multiple immune pathways.

Anti-LAP decreases LAP+ CD4 T cells and LAP+ DCs and blocks the release of TGF-β, thus restricting tolerogenic CD103+ CD8 T cells and promoting DC maturation. This leads to enhanced effector CD8+ T cell activity and the development of anti-tumor immune memory and tumor elimination.